https://doi.org/10.5194/egusphere-2026-2877
Preprint. Discussion started: 20 July 2026

Trifluoroacetic acid enhances sulfuric acid–ammonia nucleation in the cold atmosphere: Molecular mechanism and atmospheric implications

Ling Liu[1], Zizhou Cai[1], An Ning[1], Biwu Chu[2], Haotian Zu[1], Jing Li[1], Jiayi Tang[1], Xiuhui Zhang[1]

[1]*State Key Laboratory of Environment Characteristics and Effects for Near-space, Key Laboratory of Cluster Science, Ministry of Education of China, School of Chemistry and Chemical Engineering, Beijing Institute of Technology, Beijing 100081, China*
[2]*State Key Joint Laboratory of Environment Simulation and Pollution Control, Research Center for Eco-Environmental Sciences, Chinese Academy of Sciences, Beijing 100085, China*

Correspondence to: Xiuhui Zhang (zhangxiuhui@bit.edu.cn)

Abstract. New particle formation (NPF) is a major source of atmospheric particulates and cloud condensation nuclei (CCN), yet conventional sulfuric acid (SA)–ammonia (NH_3) nucleation cannot fully explain the observed NPF and CCN generation. While recent CLOUD studies have shown that nitric acid can enhance SA–NH_3 nucleation in the cold upper troposphere [Nature, 605, 483-489, 2022], this mechanism can only explain particle formation under certain cold atmospheric environments. Here, we use trifluoroacetic acid (TFA) as a model perfluorocarboxylic acid (PFCA) to investigate the stabilizing effect of PFCAs on SA–NH_3 clusters, given their atmospheric nucleation relevance, long lifetime, and widespread distribution. Using quantum chemical calculations with Atmospheric Cluster Dynamics Code simulations, we find that TFA forms stable cage-like SA–NH_3–TFA clusters via strong hydrogen bonds and proton transfer. At 220 K (favourable cold conditions), TFA enhances the SA–NH_3 nucleation rate by up to 950-fold and contributes up to 93% of the main simulated growth flux at low SA. TFA assisted stabilization represents a potentially efficient pathway for SA–NH_3 nucleation in cold atmospheres. This mechanism is most directly relevant to the cold boundary layer environments where TFA has been measured. In the upper troposphere, its role serves as a critical low-temperature mechanistic insight, pending direct observations of gas-phase TFA aloft. This study provides a molecular-level foundation for understanding general PFCA-enhanced nucleation mechanisms in cold atmospheric environments.

1 Introduction

Atmospheric new particle formation (NPF) is an important source of particulates and cloud condensation nuclei (CCN) and can influence the Earth's radiative balance and cloud properties (Gordon et al., 2017; Lee et al., 2019; Yu and Luo, 2009; Zaveri et al., 2022). Nucleation is the initial and rate-limiting step of NPF. Sulfuric acid (SA)–ammonia (NH_3) nucleation is a well-known mechanism at low temperature, but cannot adequately explain the observed particle formation events,

https://doi.org/10.5194/egusphere-2026-2877
Preprint. Discussion started: 20 July 2026

particularly under low SA conditions (Kerminen et al., 1997; Kirkby et al., 2011; Myllys et al., 2017; Williamson et al., 2019). This discrepancy indicates that additional stabilizing species may participate in the early stages of cluster formation.

Recent CLOUD (Cosmics Leaving OUtdoor Droplets) experimental studies have shown that nitric acid (NA), an important atmospheric inorganic acid, can enhance SA–NH_3 nucleation under cold atmospheric conditions (Wang et al., 2020, 2022), providing an important advance in understanding the importance of acid in upper-tropospheric particle formation. Nevertheless, the NA–SA–NH_3 nucleation may only dominates NPF in the Asian monsoon region of the upper troposphere, and NA is unlikely to be the only acidic stabilizer of SA–NH_3 clusters under cold conditions. A key unresolved question is which other atmospheric acids can provide comparable molecular stabilization and under what atmospheric conditions they may become relevant (Wang et al., 2020, 2022). Beyond inorganic acids, atmospheric organic acids (e.g., oxalic acid) can be transported to colder atmospheric regions and have been proposed to participate in low-temperature cluster formation (Bready et al., 2022; Fang et al., 2020; Lin et al., 2019; Liu et al., 2021a, 2018a; Narukawa et al., 2003; Wang et al., 2023; Zhang et al., 2018b) However, their nucleation effects depend sensitively on molecular properties, such as hydrogen-bond topology, types of intermolecular interactions, and acid/base strength (Frederiks et al., 2023; Harold et al., 2022; Nadykto and Yu, 2007; Zhang et al., 2025). Thus, identifying chemically distinct acids with stronger intrinsic cluster stabilizing ability remains an important open question for cold atmospheric nucleation.

Perfluorocarboxylic acids (PFCAs), characterized by high chemical stability and long-range atmospheric mobility, are globally distributed and differ chemically from nonhalogenated organic acids owing to their strong acidity and hydrogen-bonding capacity based on the electron-withdrawing effect of the perfluorinated alkyl groups. These properties make them promising candidates for probing acid-assisted stabilization of SA–NH_3 clusters (Prevedouros et al., 2006). As the shortest-chain, most abundant, and widely detected PFCA (Tian et al., 2018), trifluoroacetic acid (TFA) is therefore a structurally representative and ideal model compound to probe the general role of PFCAs in SA–NH_3 nucleation process in cold atmospheric environments. TFA also possesses a long atmospheric lifetime, enabling its extensive atmospheric transport and diffusion. It has been detected in both gas and particle phases in urban regions (Hu et al., 2013; Wu et al., 2014). Three-dimensional chemical transport modeling has suggested that TFA may be widely distributed across different regions. It has multiple anthropogenic sources (Freeling and Björnsdotter, 2023), including direct industrial use (López and Salazar, 2013; Xie et al., 2020) and secondary formation from the oxidative degradation of substitutes for chlorofluorocarbons (Wu et al., 2025). Emissions of gaseous TFA precursors have increased over the past decades (Freeling et al., 2022). Furthermore, the high persistence and mobility of TFA in the environment raise concerns about widespread adverse effects (Lim, 2025), making it critical to clarify its environmental impacts. Importantly, field measurements and theoretical simulations have shown that TFA can significantly enhance the atmospheric SA-dimethylamine (DMA) and methanesulfonic acid-methylamine nucleation at low temperature under diverse atmospheric boundary layer conditions (Hu et al., 2023; Liu et al., 2021b; Lu et al., 2020). These findings motivate investigating whether TFA, as a model PFCA, can also stabilize the atmospherically important SA–NH_3 nucleation system under cold atmospheric conditions.

https://doi.org/10.5194/egusphere-2026-2877
Preprint. Discussion started: 20 July 2026

The atmospheric relevance of TFA-assisted SA–NH_3 nucleation should be interpreted differently across cold atmospheric environments. The cold boundary layer provides the more directly constrained atmospheric context, because TFA has been measured in both gas and particle phases in boundary layer environments. In contrast, direct gas-phase measurements of TFA in the upper troposphere are not currently available. Therefore, the upper tropospheric calculations in this study are designed only as low-temperature sensitivity tests rather than quantitative predictions of present atmospheric particle formation. Although previous studies suggest that some PFCAs or TFA precursors may be transported to high altitudes under favorable conditions (Breuninger et al., 2025; Dodangodage et al., 2025), these lines of evidence provide only qualitative plausibility and do not constrain gas-phase TFA concentrations aloft. Accordingly, the cold boundary layer is treated here as the more observationally supported environment, whereas the upper troposphere is considered an exploratory low temperature sensitivity scenario.

Here, we use TFA as a model PFCA to investigate the ternary nucleation mechanism of $(SA)_x{\cdot}(NH_3)_y{\cdot}(TFA)_z$ ($0 \le y \le x+z \le 3$, $z = 1, 2, 3$) at the molecular scale using quantum chemical calculations combined with Atmospheric Cluster Dynamics Code (ACDC) simulations [46,47]. We first characterized the intermolecular interactions and bonding strengths within SA–NH_3–TFA clusters and then evaluated their thermodynamic stability, kinetic stability, formation rates, cluster concentrations, and dominant formation pathways under cold atmospheric conditions. In this way, the present study provides molecular-level insight into how TFA, as a model PFCA, influences the SA–NH_3 nucleation process under cold conditions, encompassing both of the cold boundary layer and the upper troposphere.

2 Theoretical methods

The structures of $(SA)_x{\cdot}(NH_3)_y{\cdot}(TFA)_z$ ($0 \le y \le x + z \le 3$, $z = 1, 2, 3$) clusters were systematically searched, and the structures of $(SA)_x{\cdot}(TFA)_z$ ($2 \le x + z \le 3$) and $(SA)_x{\cdot}(NH_3)_y$ ($1 \le y \le x \le 3$) clusters were adopted from our previous studies at the same level of theory (Liu et al., 2018b; Lu et al., 2020). The structural optimization process proceeded as follows: First, the ABCluster program (Zhang and Dolg, 2015) was used to generate the initial isomer structures of different clusters via the CHARMM36 force field. Second, up to 1000 structures with low energy were selected and optimized using the PM7 semiempirical method (Stewart, 2007) with the MOPAC 2016 software (Stewart, n.d.). Third, up to 100 structures with low energy from the above 1000 structures were further optimized at the M06-2X/6-31+G* level of theory (Zhao and Truhlar, 2008, 2011). We retained a sufficiently large number of low energy structures (usually 1,000 from CHARMM36 and 100 from PM7) at the above two stages to ensure coverage. Finally, 10 relatively stable structures were selected from the above 100 structures to be further optimized at the M06-2X/6-311++G(3df,3pd) level of theory, which has been shown to perform well for atmospherically relevant molecular clusters (Herb et al., 2011, 2013; Nadykto et al., 2011, 2009). Vibrational frequencies were also calculated for the most stable structures at the same level of theory to obtain Gibbs free energies at 240 K, 230 K, and 220 K. All the quantum chemistry calculations were performed using the Gaussian 09 package (Frisch et al., 2009).

https://doi.org/10.5194/egusphere-2026-2877
Preprint. Discussion started: 20 July 2026

Single-point energy calculations were carried out at the RI-CC2/aug-cc-pV(T+d)Z level of theory via the TURBOMOLE program (Ahlrichs et al., 1989), given the good agreement between the simulated results (cluster concentrations and cluster formation rates) based on this level of theory and the experimental and field measurements (Kürten et al., 2018; Liu et al., 2021c; Lu et al., 2020), attributed to random error cancellation (Details in Section S1 of the Supplement). Based on the ΔG calculated at RI-CC2/aug-cc-pV(T+d)Z//M06-2X/6-311++G(3df,3pd) level of theory, the ACDC (McGrath et al., 2012; Olenius et al., 2013) model was used to simulate cluster formation and derive cluster concentrations, formation rates, and relevant formation pathways (Details in Section S2 of the Supplement). Evidence for the consistency between theoretical predictions and existing experimental results is shown in Section S3 of the Supplement.

3 Results and discussion

3.1 *Cluster Structures and Intermolecular Interactions*

Intermolecular interactions are key factors in the formation of atmospheric nucleation clusters (Li et al., 2020; Zhang et al., 2025). To identify the potential interaction sites among SA, NH_3, and TFA molecules, the electrostatic potential (ESP) mapped molecular van der Waals (vdW) surfaces were analyzed at the M06-2X/6-311++G(3df,3pd) level of theory (Fig. S1). The three molecules exhibit pronounced positive and negative ESP regions, indicating their ability to form directional intermolecular interactions. The differences between the positive and negative ESP extrema of the TFA molecule and those of the SA molecule are within 2.0 kcal/mol. Given that surface electrostatic potentials are commonly employed to identify and rank hydrogen-bond donor/acceptor sites, this result suggests that TFA may exhibit a hydrogen-bonding propensity broadly comparable with SA.

Figure 1 shows the most stable structures of the $(SA)_x{\cdot}(NH_3)_y{\cdot}(TFA)_z$ ($1 \le y \le x + z \le 3$, $z \ge 1$) clusters identified in the systematic stable structure search. Cartesian coordinates are provided in Table S1 in the Supplement. Intermolecular bond lengths and the bonding positions indicate that SA, NH_3, and TFA can form cage-like clusters stabilized by the hydrogen bond network (Liu et al., 2022; Myllys et al., 2019). To further quantify the hydrogen bond strength in these clusters, the topological analysis was performed based on the atoms in molecules (AIM) theory using the Multiwfn package (Lu and Chen, 2012). As shown in Table S2, the electron density (ρ) and the corresponding Laplacian of the ρ ($\nabla^2\rho$) at the bond critical points (BCPs) of the hydrogen bonds in SA–NH_3–TFA clusters range from 0.0105 to 0.0997 a.u. and from 0.0086 to 0.1331 a.u., respectively. Most of the ρ and $\nabla^2\rho$ for the studied clusters are higher than the ranges of 0.002-0.040 a.u. and in the range of 0.014-0.139 a.u. suggested by the literature for hydrogen bond, respectively (Grabowski, 2004; Koch and Popelier, 1995). Thus, TFA can indeed form clusters with SA and NH_3 through relatively strong hydrogen bonding and electrostatic interactions.

https://doi.org/10.5194/egusphere-2026-2877
Preprint. Discussion started: 20 July 2026

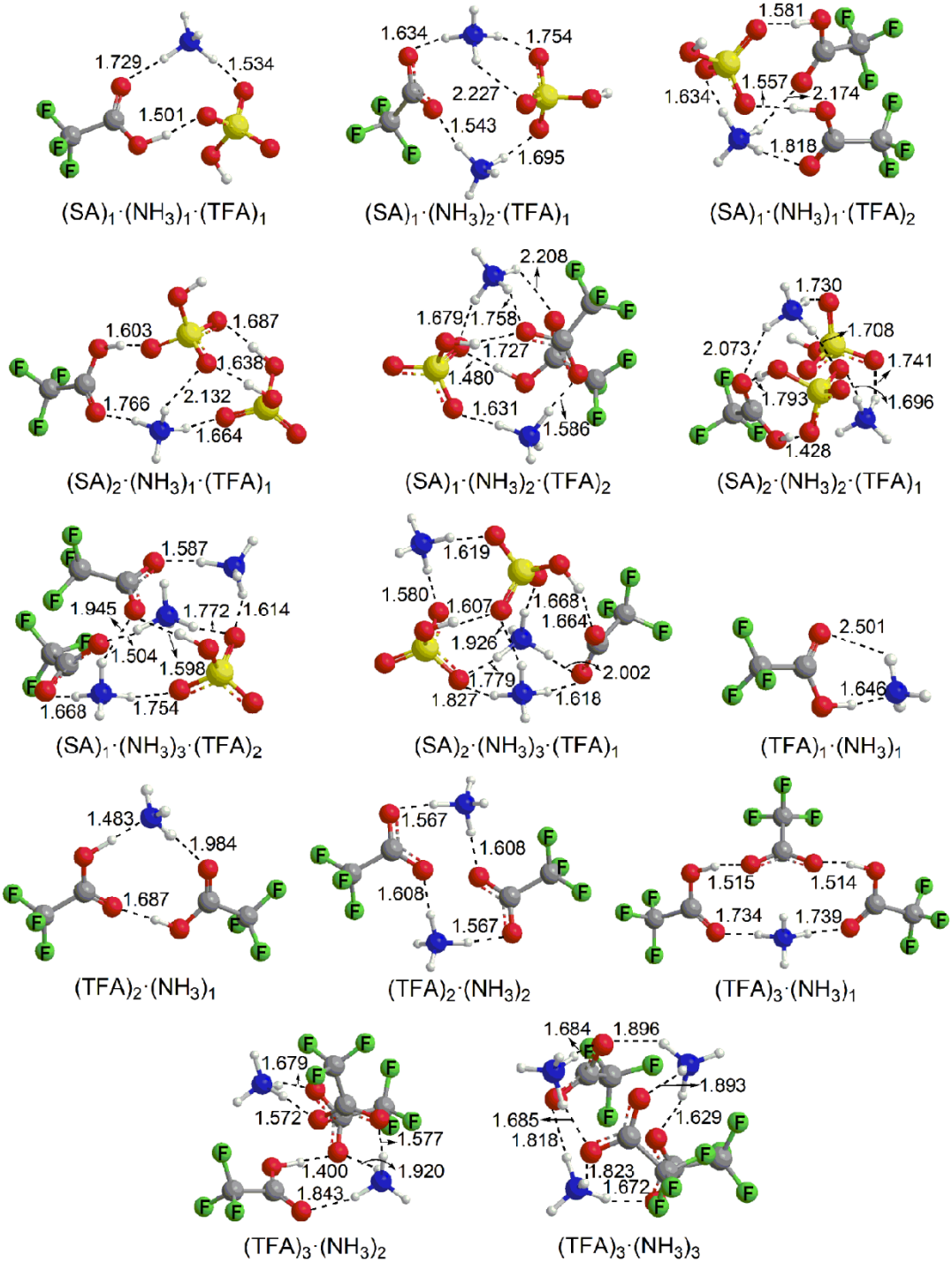

Figure 1 The most stable structures of $(SA)_x \cdot (NH_3)_y \cdot (TFA)_z$ ($0 \le y \le x+z \le 3$, $z = 1, 2, 3$) clusters. Structures were optimized at the M06-2X/6-311++G(3df,3pd) level of theory. The grey, white, red, blue, green, and yellow balls represent C, H, O, N, F, and S atoms, respectively. Dashed lines represent the hydrogen bonds. The bond lengths are in Å.

https://doi.org/10.5194/egusphere-2026-2877
Preprint. Discussion started: 20 July 2026

Proton transfer among the studied nucleation precursors was further analyzed in terms of the proton transfer parameter (Hunt et al., 2003; Kurnig and Scheiner, 1987; Liu et al., 2021c) (Section S4 in the Supplement). As shown in Table S3, proton transfer occurs in most of the studied $(SA)_x \cdot (NH_3)_y \cdot (TFA)_z$ ($0 \le y \le x+z \le 3$, z = 1, 2, 3) clusters. The number of proton transfers is equal to the number of NH_3 molecules in the clusters. Although SA exhibits a higher priority for proton transfer than TFA when both acids are present, a proton from TFA can be transferred to NH_3 when there are more NH_3 molecules than SA molecules in the clusters. Thus, TFA can stabilize SA–NH_3 nucleation clusters not only via hydrogen bonds but also by electrostatic interactions generated by proton transfer. The strong intermolecular interactions and proton transfer provide a molecular basis for the thermodynamic and kinetic stability discussed below.

3.2 Thermodynamic and Kinetic Stability of Clusters

Thermodynamic and kinetic stabilities are both critical for molecular clusters to survive evaporation and grow during atmospheric nucleation. We investigated cluster stability across temperatures (220−240 K), representative of cold atmospheric environments, including cold boundary layer and upper tropospheric conditions (Dunne et al., 2016; Wang et al., 2022). Thermodynamic stability of SA–NH_3–TFA clusters was evaluated via the Gibbs free energies of formation (ΔG), which is defined as the G of the cluster relative to the sum G of the corresponding constituent monomers. The ΔG values are all negative for the studied clusters involving TFA at the studied temperatures (Table S4), a result that indicates the formation of these clusters is thermodynamically favorable. The ΔG values of the SA–NH_3–TFA clusters decrease as temperature decreases. Hence, SA–NH_3–TFA clusters are predicted to become more thermodynamically stable at lower temperatures. This trend supports the potential importance of TFA assisted stabilization in the cold boundary layer environments and the upper tropospheric sensitivity scenarios. The effect of anharmonicity on the calculated Gibbs free energy was examined using a Zero Point Energy (ZPE) scaling factor of 0.97 (Alecu et al., 2010). As shown in Table S5, the deviation in the calculated Gibbs free energy of cluster formation (ΔG) between the calculations with a ZPE scaling factor of 0.97 and those without scaling corrections is within 2.2 kcal/mol. This uncertainty is further considered when interpreting the absolute values of cluster formation rates.

Kinetic stability, reflected in the growth trend, is determined by the ratio ($\beta \cdot C/\sum\gamma$) of collision frequency ($\beta \cdot C$, β shown in Table S6) with a monomer molecule to total evaporation frequency ($\sum\gamma$, Table S7) of all possible monomer evaporations. If the $\beta \cdot C$ of a cluster is higher than its $\sum\gamma$, the cluster is more likely to grow into larger clusters than to evaporate. To assess the growth tendency of SA–NH_3–TFA clusters under low temperatures, we analyzed the $\beta \cdot C/\sum\gamma$ at low concentrations of the corresponding nucleation precursors and different temperatures (240 K, 230 K, and 220 K) (Table S8). For example, at relative low nucleation precursor concentration of 1.0×10^6 molecules cm^{-3}, the $\beta \cdot C/\sum\gamma$ of the $(SA)_x \cdot (NH_3)_y \cdot (TFA)_1$ clusters ($0 \le x \le 2$, $1 \le y \le 3$, $y \le x+1$) increases markedly as temperature decreases (Fig. 2). The $\beta \cdot C/\sum\gamma$ of $(SA)_2 \cdot (NH_3)_3 \cdot (TFA)_1$ cluster increases from 1.4 at 240 K to 1.3×10^2 at 220 K. This indicates that lower temperature favors cluster growth over monomer evaporation. (Details in Section S5 of the Supplement). This temperature dependence arises because evaporation

https://doi.org/10.5194/egusphere-2026-2877
Preprint. Discussion started: 20 July 2026

frequencies decrease more strongly with decreasing temperature than collision frequencies, allowing TFA containing clusters to survive and grow more efficiently. Overall, both thermodynamic and kinetic analyses show that SA–NH_3–TFA clusters become increasingly stable under colder conditions.

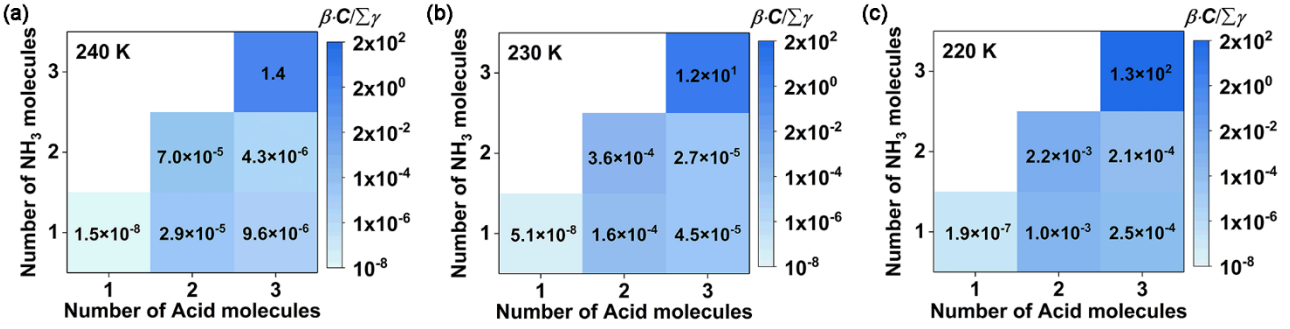

Figure 2 Ratios of SA monomer collision frequencies to total evaporation frequencies ($\beta \cdot C/\sum\gamma$) for $(SA)_x \cdot (NH_3)_y \cdot (TFA)_1$ ($0 \le x \le 2$, $1 \le y \le 3$, $y \le x+1$) clusters at different temperatures. (a) 240 K, (b) 230 K, and (c) 220 K. $C = 1.0 \times 10^6$ molecules cm^{-3}.

3.3 Particle Formation Rates Enhanced by TFA

Given that TFA can form stable clusters with SA and NH_3, we further investigated the particle formation rates (J) of SA–NH_3–TFA nucleation process. The J of SA–NH_3–TFA nucleation mechanism and the enhancement (R_J) of SA–NH_3 nucleation by TFA were analyzed in a wide range of common nucleation precursor concentrations ([SA] = 7.0×10^5–1.0×10^7 molecules cm^{-3} (Kürten et al., 2012; Yao et al., 2018; Zheng et al., 2015), [NH_3] = 1.0×10^8–1.0×10^{11} molecules cm^{-3} (Bray et al., 2017; Höpfner et al., 2019; You et al., 2014)). These ranges cover values relevant to boundary layer environments and upper tropospheric sensitivity conditions, although their representativeness differs among atmospheric environments. The TFA concentrations adopted here (1.0×10^6 to 1.0×10^8 molecules cm^{-3}) are referenced to field measurements in the boundary layer (Wu et al., 2014; Zhang et al., 2018a). Direct observational constraints on TFA concentrations in the upper troposphere are currently unavailable. We therefore do not assign an observationally constrained TFA abundance to this region. It should be regarded strictly as an exploratory sensitivity range used to study the potential effect of TFA if it were present aloft at comparable gas-phase concentrations. Accordingly, the simulated upper-tropospheric formation rates should be interpreted as scenario-based sensitivity results rather than as quantitative predictions for the present atmosphere (Details in Sections S6 and S7 of the Supplement). The simulations were performed at 240, 230, and 220 K, with condensation sinks (CSs) of 2.0×10^{-2}, and 2.0×10^{-3} s^{-1}. Taking the temperature of 240 K as an example, the particle formation rate (J) calculated using anharmonicity corrected ΔG (Fig. S2) is about 1.1 times that obtained with the harmonic approximation. Given the relatively insignificant impact of the anharmonicity on the simulated results, the harmonic approximation was adopted for all the computed data in this study.

Across the examined precursor concentration ranges, both J and R_J increase as temperature decreases (Fig. 3). This indicates that the enhancement of SA–NH_3 nucleation by TFA becomes stronger at lower temperatures. Moreover, J increases with increasing [SA] [Fig. 3 (a)], whereas R_J exhibits the opposite trend, increasing as [SA] decreases [Fig. 3 (b)].

https://doi.org/10.5194/egusphere-2026-2877
Preprint. Discussion started: 20 July 2026

At medium [NH_3] (1.0×10^{10} molecules cm^{-3}), medium [TFA] (1.0×10^{7} molecules cm^{-3}), and 220 K, R_J reaches 46-fold at low [SA] (7.0×10^{5} molecules cm^{-3}) [blue dashed line, Fig. 3 (b)]. This highlights that the enhancement of the SA–NH_3 nucleation by TFA becomes increasingly significant under low [SA] conditions with effective sulfur emission controls. Both J and R_J increase with increasing [NH_3] [Figs. 3 (c) and 3 (d)]. At the low [SA] (7.0×10^{5} molecules cm^{-3}), medium [TFA] (1.0×10^{7} molecules cm^{-3}), R_J reaches 55-fold at high [NH_3] (1.0×10^{11} molecules cm^{-3}) and 220 K [Fig. 3 (d)]. These results indicate that the enhancement of SA–NH_3 nucleation by TFA can be pronounced in cold regions with high NH_3 levels, such as regions affected by agricultural and pastoral emissions or efficient vertical transport of boundary layer NH_3. Additionally, both J and R_J increase with increase of [TFA] [Figs. 3 (e) and 3 (f)]. At low [SA] (7.0×10^{5} molecules cm^{-3}), high [NH_3] (1.0×10^{11} molecules cm^{-3}), R_J can be up to 9.5×10^{2} at high [TFA] (1.0×10^{8} molecules cm^{-3}) and 220 K [Fig. 3 (f)]. These results suggest that TFA strongly enhances SA–NH_3 nucleation in the cold regions with low [SA] but high [NH_3] or [TFA]. These results suggest that SA–NH_3–TFA nucleation may become increasingly relevant under low [SA] conditions if gas-phase TFA is sufficiently abundant. Quantifying its contribution to NPF and CCN formation, however, requires observational constraints and regional or global aerosol modeling.

CS varies with the abundance of atmospheric background particles. We therefore further examined J and R_J at relatively low CS of 2.0×10^{-3} s^{-1}, representative of clean areas (Fig. S3). J at CS = 2.0×10^{-3} s^{-1} is much higher than that at CS = 2.0×10^{-2} s^{-1}. For instance, J increases from 9.1 cm^{-3} s^{-1} to 1.6×10^{3} cm^{-3} s^{-1} when CS decreases from 2.0×10^{-2} s^{-1} to 2.0×10^{-3} s^{-1} at [SA] = 7.0×10^{5} molecules cm^{-3}, [NH_3] = 1.0×10^{11} molecules cm^{-3}, [TFA] = 1.0×10^{8} molecules cm^{-3}, and 220 K. Although R_J varies with CS under different temperatures and nucleation precursor concentrations, the variation magnitude is small (within 5-fold). This indicates the relative enhancement by TFA is less sensitive to CS than the absolute formation rate within the examined CS range.

Water vapor is ubiquitous in the atmosphere and pressure varies with increasing altitude. They may also influence atmospheric cluster formation. Our theoretical calculations reveal that variations in relative humidity and pressure have smaller effects on the calculated SA–NH_3–TFA formation rates than temperatures and precursor concentrations. Details are provided in the Section S8 of the Supplement.

https://doi.org/10.5194/egusphere-2026-2877
Preprint. Discussion started: 20 July 2026

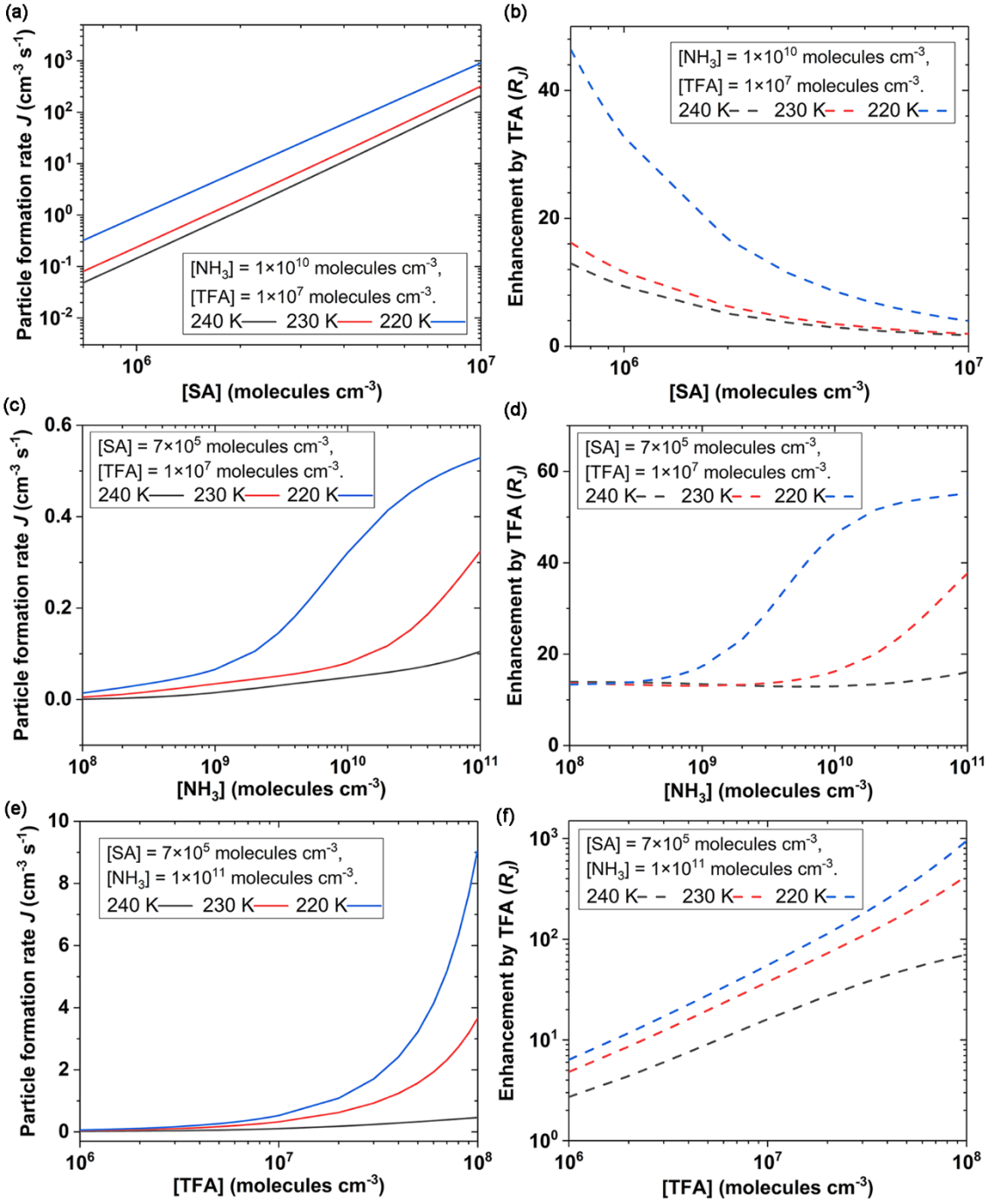

Figure 3 Particle formation rates (J, cm^{-3} s^{-1}) and enhancement on particle formation rate by TFA (R_J, $R_J = J_{SA–NH3–TFA}/J_{SA–NH3}$) at different temperatures and nucleation precursor concentrations. Black, red, and blue lines correspond to the J at 240 K, 230 K, and 220 K, respectively. CS = 2.0 × 10^{-2} s^{-1}.

https://doi.org/10.5194/egusphere-2026-2877
Preprint. Discussion started: 20 July 2026

3.4 Cluster Concentrations and Enhancement

Cluster concentration is another key parameter in the particle formation process. To assess the influence of TFA on cluster concentrations, we analyzed the cluster concentrations of SA–NH_3–TFA based nucleation system under different nucleation precursor concentrations (SA, NH_3, and TFA) and temperatures. Concentrations of SA–NH_3–TFA clusters with different numbers of molecules increase with increasing [SA] [Fig. 4 (a)], [NH_3] [Fig. 4 (c)] and [TFA] [Fig. 4 (e)]. For instance, the concentrations of the smallest clusters with two molecules and the largest clusters with six molecules can be up to 4.4×10^5 molecules cm^{-3} and 1.1×10^3 molecules cm^{-3}, respectively, at high [TFA] (1.0×10^8 molecules cm^{-3}) and 240 K [Fig. 4 (e)]. In addition, cluster concentrations decrease with increasing temperature at the different concentrations of nucleation precursors. At [TFA] = 1.0×10^8 molecules cm^{-3}, the concentration of clusters with two molecules and with six molecules can increase from 4.4×10^5 molecules cm^{-3} to 2.7×10^6 molecules cm^{-3} and from 1.1×10^3 molecules cm^{-3} to 4.2×10^4 molecules cm^{-3}, respectively, with the temperature decreasing from 240 K to 220 K. These trends indicate that the contribution of TFA to cluster concentrations becomes more pronounced as temperature decreases. This temperature dependence is directly relevant to the conditions of the cold boundary layer, where TFA is observationally better constrained and low-SA/high-NH_3 conditions may favor efficient cluster production, and it may also be important under cold upper tropospheric conditions, where low temperature can strongly stabilize clusters.

The influence of TFA on the cluster concentrations in the SA–NH_3-based nucleation system was further studied [Figs. 4 (b), (d), and (f)]. TFA participation substantially enhances cluster concentrations, with the enhancement (R_C) showing a negative correlation with [SA] and temperature, and positive correlation with [NH_3] and [TFA]. As shown in Fig. 4 (f), TFA enhances the concentration of the smallest clusters (two-molecule) by up to 4-fold and the largest clusters (six molecule) clusters by 1.3×10^3-fold at low [SA] (7.0×10^5 molecules cm^{-3}) and temperature (220 K), high [NH_3] (1.0×10^{11} molecules cm^{-3}) and [TFA] (1.0×10^8 molecules cm^{-3}). This highlights that TFA contributes strongly to cluster abundances in the SA–NH_3 system, particularly under conditions of low [SA], low temperatures, and high [NH_3] or [TFA].

Comparison of results at CS = 2.0×10^{-2} s^{-1} and CS = 2.0×10^{-3} s^{-1} (Fig. S4) shows that cluster concentrations increase and R_C decreases slightly as CS decreases. The effects of temperature and nucleation precursor concentrations on cluster concentrations and R_C at CS = 2.0×10^{-3} s^{-1} are largely consistent with those at CS = 2.0×10^{-2} s^{-1}. These trends indicate that TFA's enhancement on cluster concentrations in SA–NH_3-based nucleation system is most pronounced in the low temperature, low [SA] but high [NH_3], high [TFA], and high CS cases examined here.

https://doi.org/10.5194/egusphere-2026-2877
Preprint. Discussion started: 20 July 2026

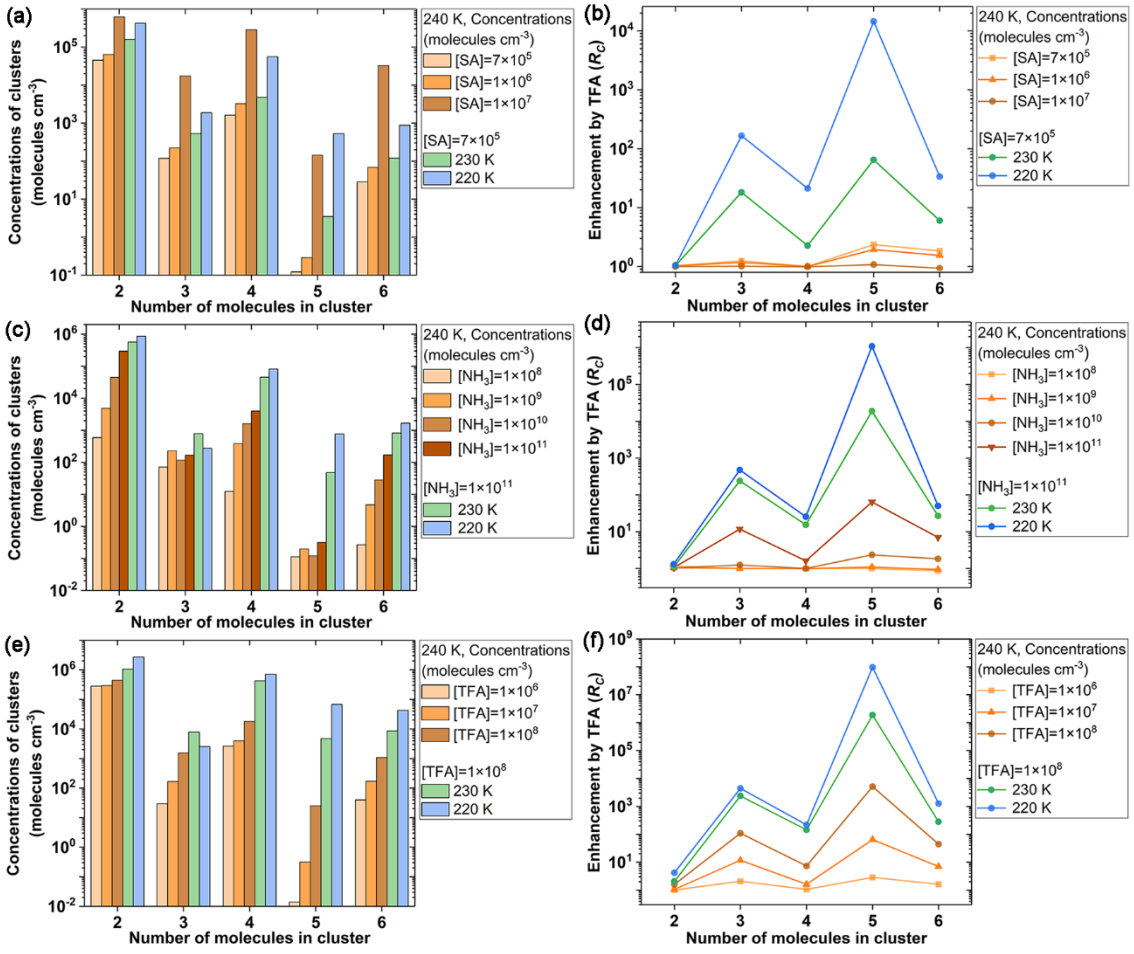

Figure 4 Cluster concentrations (molecules cm^{-3}) and enhancement on concentrations of clusters by TFA (R_C, $R_C = C_{SA–NH3–TFA}/C_{SA–NH3}$) at different temperatures. CS = 2.0×10^{-2} s^{-1}. (a) and (b): $[NH_3] = 1.0 \times 10^{10}$ molecules cm^{-3}, $[TFA] = 1.0 \times 10^7$ molecules cm^{-3}. (c) and (d): $[SA] = 7.0 \times 10^5$ molecules cm^{-3}, $[TFA] = 1.0 \times 10^7$ molecules cm^{-3}. (e) and (f): $[SA] = 7.0 \times 10^5$ molecules cm^{-3}, $[NH_3] = 1.0 \times 10^{11}$ molecules cm^{-3}.

3.5 Dominant Cluster Formation Pathways

To clarify the molecular growth mechanism, we simulated the formation pathways of the SA–NH_3–TFA clusters at median nucleation precursor concentrations and different temperatures (220 K, 230 K, and 240 K). Fig. 5 identifies two main cluster formation pathways, one involving TFA (blue arrows) and the other excluding TFA (grey arrows). The main cluster formation pathways are identical at 240 K and 230 K as shown by all the blue and grey arrows, while pathways covered by the light grey shadow (contribution ≤ 5%) are absent at 220 K. Detailed contributions of each pathway to the corresponding larger clusters are shown in Fig. S5. The contributions of pathways covered by the light grey shadow to the formation of the relevant larger clusters are smaller than that of the corresponding alternative pathways at 240 K and 230 K.

https://doi.org/10.5194/egusphere-2026-2877
Preprint. Discussion started: 20 July 2026

Since the cluster formation pathways with contributions lower than 5% are excluded in Fig. 5, the total contributions as shown in the Figs. 5 (b) and (c) are not 100%. To clarify the contribution variation trend with temperature, the contributions lower than 5% of TFA-free pathways are shown in Fig. 5(c). Within the simulated neutral cluster system, contributions of TFA-involved pathways (the formation pathway of $(SA)_2{\cdot}(NH_3)_3{\cdot}(TFA)_1$ cluster, blue histograms) to the main cluster formation pathways increase from 53% to 93% when the temperature decreases from 240 K to 220 K. Conversely, the contributions of TFA-free pathways (grey histograms) to the main cluster formation pathways increase with rising temperature. This occurs because lower temperatures enhance J more strongly in the SA–NH_3–TFA system than in the binary SA–NH_3 system, which is in accordance with the increasing enhancement of TFA on SA–NH_3 nucleation as temperature decreases (Fig. 3).

We further examined how precursor concentrations affect the relative contributions of TFA-involved and TFA-free pathways to the main cluster formation pathway. Table S9 shows that contribution variation trends with temperatures of different cluster formation pathways are the same at different [SA], [NH_3], and [TFA]. At a given temperature, the contribution of cluster formation involving TFA increases with the decrease of [SA] and the increase of [NH_3] or [TFA]. In summary, TFA-containing pathways can dominate the simulated SA–NH_3–TFA growth flux under low temperature, low [SA], high [NH_3], and high [TFA] conditions. This mechanism is directly relevant in the cold boundary layer environments and may also be relevant to the upper troposphere if sufficient TFA is transported or produced aloft.

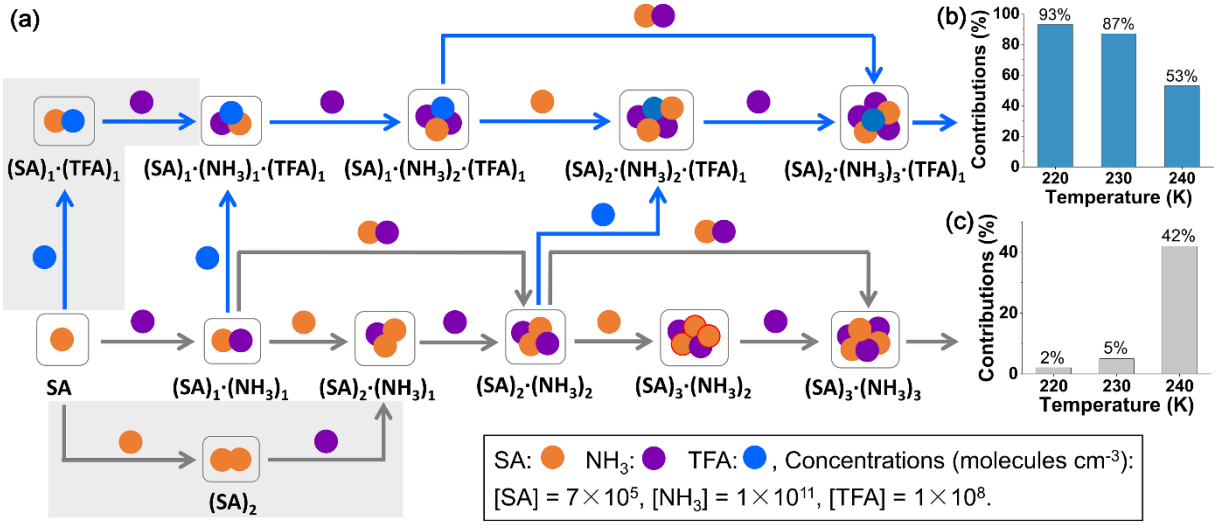

Figure 5 (a) Main cluster formation pathways of SA–NH_3–TFA clusters at [SA] = 7.0 × 10^5 molecules cm^{-3}, [NH_3] = 1.0 × 10^{11} molecules cm^{-3}, and [TFA] = 1.0 × 10^8 molecules cm^{-3}. Blue arrows show the pathways involving TFA and grey arrows show the pathways without TFA. The pathways covered by the light grey shadow are only present at 240 K and 230 K, but not present at 220 K. Pathways not shaded in light grey occur at all three temperatures (240 K, 230 K, and 220 K). The histograms show the contributions of pathways (b) involving TFA and (c) without TFA to the main cluster formation pathway at different temperatures (240 K, 230 K, and 220 K).

https://doi.org/10.5194/egusphere-2026-2877
Preprint. Discussion started: 20 July 2026

3.6 Atmospheric relevance in the cold boundary layer and upper troposphere

To elucidate the atmospheric relevance of SA–NH_3–TFA nucleation mechanism, we compare it across two cold atmospheric environments with different levels of observational constraint. The cold boundary layer represents the more directly constrained atmospheric setting because TFA has been measured in atmospheric boundary layer. In contrast, the upper tropospheric analysis aims to assess whether the SA–NH_3–TFA mechanism could become important if TFA was present aloft, given that direct gas-phase TFA measurements in this region are not yet available.

For the cold boundary layer, Fig. 6(a) compares the simulated J of SA–NH_3–TFA (red line for $[NH_3] = 2.0 \times 10^{10}$ molecules cm^{-3} and blue line for $[NH_3] = 5.0 \times 10^{10}$ molecules cm^{-3}) nucleation mechanism with that of the well-established SA-DMA mechanism (black line) under cold polluted boundary layer conditions. Here, the relevance of TFA is more directly connected to existing observations, because TFA has already been measured in the atmospheric boundary layer. Under low [SA] ($< 1.0 \times 10^6$ molecules cm^{-3}) and relatively high $[NH_3]$, the J of SA–NH_3–TFA is slightly higher than that of SA-DMA at $[NH_3] = 2.0 \times 10^{10}$ molecules cm^{-3}, and can be up to five times higher when $[NH_3] = 5.0 \times 10^{10}$ molecules cm^{-3} and $[SA] = 7.0 \times 10^5$ molecules cm^{-3}. This comparison suggests that the SA–NH_3–TFA nucleation can be competitive with the SA-DMA nucleation in the cold boundary layer, especially under low [SA] and elevated $[NH_3]$ conditions.

For the upper troposphere, Fig. 6(b) compares the simulated J values of the SA–NH_3–TFA mechanism (red line) with those of the SA–NH_3–NA mechanism (black line) under selected upper tropospheric sensitivity conditions. Although the J of SA–NH_3–TFA is slightly lower than that of SA–NH_3–NA at low $[NH_3]$, it becomes comparable to or higher than that of SA–NH_3–NA at high $[NH_3]$ ($> 2.0 \times 10^9$ molecules cm^{-3}) and prescribed high [TFA] (2.0×10^7 molecules cm^{-3}–1.0×10^8 molecules cm^{-3}, green areas in Fig. 6(b)). At $[NH_3]$ of 1.0×10^{10} molecules cm^{-3}, the J of SA–NH_3–TFA can be four times higher than that of SA–NH_3–NA. These results suggest that, if TFA is present aloft at sufficient abundance (higher than 2.0×10^7 molecules cm^{-3}), the SA–NH_3–TFA pathway can compete with or exceed SA–NH_3–NA nucleation in cold upper troposphere. Even at a considerably low [TFA] of 1.0×10^5 molecules cm^{-3}, the J of SA–NH_3–TFA system is still 17 times higher than that of SA–NH_3–NA system an equally low [SA] of 1.0×10^5 molecules cm^{-3} (Fig. S6). These highlight PFCAs may be previously unrecognized stabilizers in the upper troposphere. These results provide testable hypotheses for assessing the nucleation potential of TFA in the upper troposphere when TFA is present aloft. Taken together, Fig. 6 illustrates two distinct interpretations of the SA–NH_3–TFA mechanism: one is observationally supported by measured TFA concentrations in the cold boundary layer, while the other represents as a mechanistically informative low-temperature test for the upper troposphere, where low temperatures strongly amplify the enhancement provided that gaseous TFA is present.

https://doi.org/10.5194/egusphere-2026-2877
Preprint. Discussion started: 20 July 2026

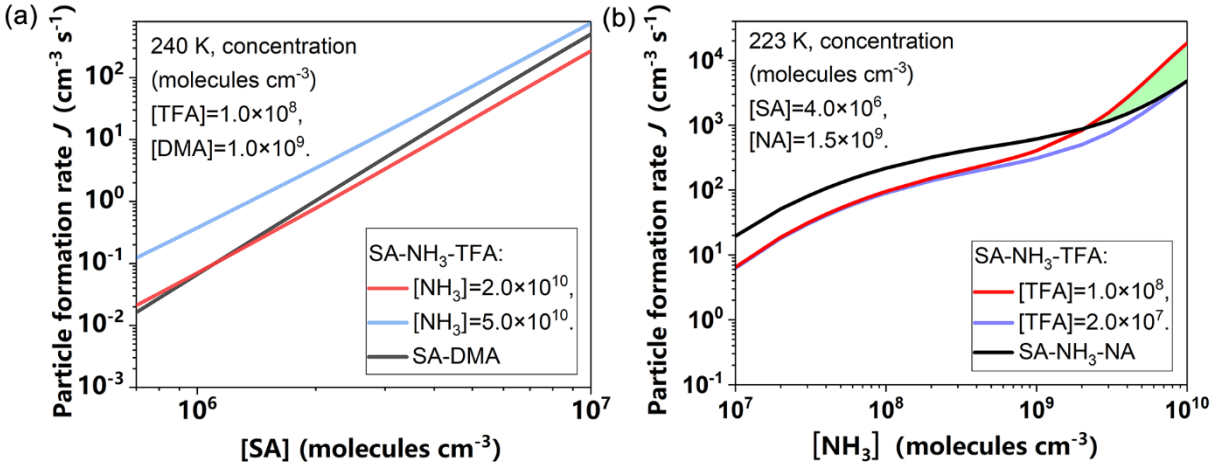

Figure 6 Atmospheric relevance of SA–NH_3–TFA nucleation across two cold atmospheric environments. (a) Comparison of particle formation rates (J, cm^{-3} s^{-1}) between SA–NH_3–TFA and SA-DMA under cold polluted boundary layer conditions as a function of [SA] at 240 K. Blue and red lines show the J for SA–NH_3–TFA at [NH_3] = 2.0 × 10^{10} molecules cm^{-3} and 5.0 × 10^{10} molecules cm^{-3}, respectively. Black line shows the J for SA-DMA. [TFA] = 1.0 × 10^8 molecules cm^{-3}, [DMA] = 1.0 × 10^9 molecules cm^{-3}. (b) Comparison of particle formation rates (J, cm^{-3} s^{-1}) between SA–NH_3–TFA and SA–NH_3–NA under selected upper tropospheric sensitivity conditions as a function of [NH_3] at 223 K. Blue and red lines show the J for SA–NH_3–TFA at the concentration of TFA at 1.0 × 10^8 molecules cm^{-3} and 2.0 × 10^7 molecules cm^{-3}, respectively. Black line shows the J for SA–NH_3–NA. [SA] = 4.0 × 10^6 molecules cm^{-3}, [NA] = 1.5 × 10^9 molecules cm^{-3}.

4 Conclusions

In this study, TFA was used as a model PFCA to investigate how a halogenated organic acid influences SA–NH_3 nucleation at the molecular scale. The results show that TFA forms stable cage-like clusters with SA and NH_3 through interaction networks of strong hydrogen bonds and electrostatic interactions arising from proton transfer. Hence, beyond the SA–NH_3 binary nucleation mechanism, the SA–NH_3–TFA ternary mechanism emerges as a particularly critical contributor to the clustering process.

The thermodynamic stability and kinetic growth tendency of SA–NH_3–TFA clusters increase as temperature decreases. Accordingly, both the particle formation rates (J) and cluster number concentrations increase under colder conditions. The enhancement of the J and cluster concentrations (R_J and R_C) for SA–NH_3 nucleation by TFA are stronger at lower temperatures and lower [SA], but increase with [NH_3] and [TFA]. The R_J and R_C can be up to 9.5 × 10^2-fold and 1.3 × 10^3-fold, respectively, and the contribution of the SA–NH_3–TFA ternary nucleation mechanism to the main clustering pathways can be up to 93% at 220 K under conditions of low [SA], high [NH_3], and high [TFA] conditions. Thus, under the cold atmospheric scenarios considered here, TFA can significantly enhance and extensively participate under the SA–NH_3 nucleation, particularly at low [SA], and elevated [NH_3] and [TFA]. The mechanism has different levels of atmospheric support in different cold atmospheric environments. It is directly relevant in the cold boundary layer, where TFA has been observed. In the upper troposphere, the results represent a robust mechanistic low-temperature sensitivity tests that demonstrates how strongly low temperatures amplify TFA-assisted nucleation, should TFA be present aloft. Several

https://doi.org/10.5194/egusphere-2026-2877
Preprint. Discussion started: 20 July 2026

limitations define the scope of inference of this study. First, TFA is used here as a model PFCA rather than as a concentration-based proxy for all PFCAs, because individual PFCAs differ in abundance, transport, and chemical formation. Second, this study identifies nucleation potential and its dependence on temperatures and precursor concentrations, but it does not quantify the net contribution of this mechanism to regional or global atmospheric particulates and CCN budgets.

Overall, this work provides molecular-level evidence that TFA, as a representative model PFCA, can efficiently stabilize SA–NH_3 cluster and enhance nucleation under cold atmospheric conditions. The findings extend current understanding of acid enhanced atmospheric clustering involving halogenated organic acids and provide testable hypotheses for future measurements and chamber experiments. Future work should prioritize chamber studies under controlled low temperatures, simultaneous field measurements of gas phase TFA, SA, NH_3, and particles in cold boundary-layer environments, direct measurements of gas phase TFA and related PFCAs aloft, and regional or global aerosol modeling to evaluate whether this mechanism contributes measurably to atmospheric NPF and CCN populations.

Data availability

The data in this article are available from the corresponding author upon reasonable request (zhangxiuhui@bit.edu.cn).

Author contributions

XZ designed and supervised the research. LL and ZC performed the quantum chemical calculations and the ACDC simulations. LL, ZC, and XZ analyzed data. LL and XZ wrote the manuscript. LL, ZC, AN, BC, HZ, JL, JT, and XZ reviewed and edited the manuscript. All authors commented on the paper.

Competing interests

The contact author has declared that neither they nor their co-authors have any competing interests.

Disclaimer

Publisher's note: Copernicus Publications remains neutral with regard to jurisdictional claims in published maps and institutional affiliations.

https://doi.org/10.5194/egusphere-2026-2877
Preprint. Discussion started: 20 July 2026

Acknowledgements

This work was supported by the National Science Fund for Distinguished Young Scholars [grant number 22225607] and the National Natural Science Foundation of China [grant numbers 22376013 and 22306011]. L. Liu thanks the Beijing Institute of Technology Research Fund Program for Young Scholars. We thank for the technical support of the National Large Scientific and Technological Infrastructure "Earth System Numerical Simulation Facility" (https://cstr.cn/31134.02.EL).

Financial support

This work was supported by the National Science Fund for Distinguished Young Scholars [grant number 22225607] and the National Natural Science Foundation of China [grant numbers 22376013 and 22306011]. L. Liu thanks the Beijing Institute of Technology Research Fund Program for Young Scholars.

References

Ahlrichs, R., Bär, M., Häser, M., Horn, H., and Kölmel, C.: Electronic structure calculations on workstation computers: The program system turbomole, Chem. Phys. Lett., 162, 165–169, https://doi.org/10.1016/0009-2614(89)85118-8, 1989.

Alecu, I. M., Zheng, J., Zhao, Y., and Truhlar, D. G.: Computational thermochemistry: Scale factor databases and scale factors for vibrational frequencies obtained from electronic model chemistries, J. Chem. Theory Comput., 6, 2872–2887, https://doi.org/10.1021/ct100326h, 2010.

Bray, C. D., Battye, W., Aneja, V. P., Tong, D., Lee, P., Tang, Y., and Nowak, J. B.: Evaluating ammonia (NH3) predictions in the NOAA National Air Quality Forecast Capability (NAQFC) using in situ aircraft, ground-level, and satellite measurements from the DISCOVER-AQ Colorado campaign, Atmos. Environ., 163, 65–76, https://doi.org/10.1016/j.atmosenv.2017.05.032, 2017.

Bready, C. J., Vanovac, S., Odbadrakh, T. T., and Shields, G. C.: Amino acids compete with ammonia in sulfuric acid-based atmospheric aerosol prenucleation: The case of glycine and serine, J. Phys. Chem. A, 126, 5195–5206, https://doi.org/10.1021/acs.jpca.2c03539, 2022.

Breuninger, A., Joppe, P., Wilsch, J., Schwenk, C., Bozem, H., Emig, N., Merkel, L., Rossberg, R., Keber, T., Kutschka, A., Waleska, P., Hofmann, S., Richter, S., Ungeheuer, F., Dörholt, K., Hoffmann, T., Miltenberger, A., Schneider, J., Hoor, P., and Vogel, A. L.: Organic aerosols mixing across the tropopause and its implication for anthropogenic pollution of the UTLS, Atmos. Chem. Phys., 25, 16533–16551, https://doi.org/10.5194/acp-25-16533-2025, 2025.

Dodangodage, R., Bernath, P. F., Boone, C., Harrison, J. J., Lecours, M., Schmidt, M., Montzka, S. A., Vimont, I., and Crotwell, M.: The first satellite measurements of HFC-125 by the ACE-FTS: Long-term trends and distribution in the Earth's upper troposphere and lower stratosphere, J. Quant. Spectrosc. Radiat. Transf., 330, 109218, https://doi.org/10.1016/j.jqsrt.2024.109218, 2025.

https://doi.org/10.5194/egusphere-2026-2877
Preprint. Discussion started: 20 July 2026

Dunne, E. M., Gordon, H., Kürten, A., Almeida, J., Duplissy, J., Williamson, C., Ortega, I. K., Pringle, K. J., Adamov, A., Baltensperger, U., Barmet, P., Benduhn, F., Bianchi, F., Breitenlechner, M., Clarke, A., Curtius, J., Dommen, J., Donahue, N. M., Ehrhart, S., Flagan, R. C., Franchin, A., Guida, R., Hakala, J., Hansel, A., Heinritzi, M., Jokinen, T., Kangasluoma, J., Kirkby, J., Kulmala, M., Kupc, A., Lawler, M. J., Lehtipalo, K., Makhmutov, V., Mann, G., Mathot, S., Merikanto, J., Miettinen, P., Nenes, A., Onnela, A., Rap, A., Reddington, C. L. S., Riccobono, F., Richards, N. A. D., Rissanen, M. P., Rondo, L., Sarnela, N., Schobesberger, S., Sengupta, K., Simon, M., Sipilä, M., Smith, J. N., Stozkhov, Y., Tomé, A., Tröstl, J., Wagner, P. E., Wimmer, D., Winkler, P. M., Worsnop, D. R., and Carslaw, K. S.: Global atmospheric particle formation from CERN CLOUD measurements, Science, 354, 1119–1124, https://doi.org/10.1126/science.aaf2649, 2016.

Fang, X., Hu, M., Shang, D., Tang, R., Shi, L., Olenius, T., Wang, Y., Wang, H., Zhang, Z., Chen, S., Yu, X., Zhu, W., Lou, S., Ma, Y., Li, X., Zeng, L., Wu, Z., Zheng, J., and Guo, S.: Observational evidence for the involvement of dicarboxylic acids in particle nucleation, Environ. Sci. Technol. Lett., 7, 388–394, https://doi.org/10.1021/acs.estlett.0c00270, 2020.

Frederiks, N. C., Hariharan, A., and Johnson, C. J.: Spectroscopic Studies of Clusters of Atmospheric Relevance, Annu. Rev. Phys. Chem., 74, 99–121, https://doi.org/10.1146/annurev-physchem-062322-041503, 2023.

Freeling, F. and Björnsdotter, M. K.: Assessing the environmental occurrence of the anthropogenic contaminant trifluoroacetic acid (TFA), Curr. Opin. Green Sustain. Chem., 41, 100807, https://doi.org/10.1016/j.cogsc.2023.100807, 2023.

Freeling, F., Scheurer, M., Koschorreck, J., Hoffmann, G., Ternes, T. A., and Nödler, K.: Levels and temporal trends of trifluoroacetate (TFA) in archived plants: Evidence for increasing emissions of gaseous TFA precursors over the last decades, Environ. Sci. Technol. Lett., 9, 400–405, https://doi.org/10.1021/acs.estlett.2c00164, 2022.

Frisch, M. J., Trucks, G. W., Schlegel, H. B., Scuseria, G. E., Robb, M. A., Cheeseman, J. R., Scalmani, G., Barone, V., Mennucci, B., Petersson, G. A., Nakatsuji, H., Caricato, M., Li, X., Hratchian, H. P., Izmaylov, A. F., Bloino, J., Zheng, G., Sonnenberg, J. L., Hada, M., Ehara, M., Toyota, K., Fukuda, R., Hasegawa, J., Ishida, M., Nakajima, T., Honda, Y., Kitao, O., Nakai, H., Vreven, T., Montgomery, J. A., Peralta, J. E., Ogliaro, F., Bearpark, M., Heyd, J. J., Brothers, E., Kudin, K. N., Staroverov, V. N., Kobayashi, R., Normand, J., Raghavachari, K., Rendell, A., Burant, J. C., Iyengar, S. S., Tomasi, J., Cossi, M., Rega, N., Millam, J. M., Klene, M., Knox, J. E., Cross, J. B., Bakken, V., Adamo, C., Jaramillo, J., Gomperts, R., Stratmann, R. E., Yazyev, O., Austin, A. J., Cammi, R., Pomelli, C., Ochterski, J. W., Martin, R. L., Morokuma, K., Zakrzewski, V. G., Voth, G. A., Salvador, P., Dannenberg, J. J., Dapprich, S., Daniels, A. D., Farkas, O., Foresman, J. B., Ortiz, J. V, Cioslowski, J., and Fox, D. J.: Gaussian 09, Revision A.1, Gaussian Inc., Wallingford CT, 2009.

Gordon, H., Kirkby, J., Baltensperger, U., Bianchi, F., Breitenlechner, M., Curtius, J., Dias, A., Dommen, J., Donahue, N. M., Dunne, E. M., Duplissy, J., Ehrhart, S., Flagan, R. C., Frege, C., Fuchs, C., Hansel, A., Hoyle, C. R., Kulmala, M., Kürten, A., Lehtipalo, K., Makhmutov, V., Molteni, U., Rissanen, M. P., Stozkhov, Y., Tröstl, J., Tsagkogeorgas, G., Wagner, R., Williamson, C., Wimmer, D., Winkler, P. M., Yan, C., and Carslaw, K. S.: Causes and importance of new particle formation in the present-day and preindustrial atmospheres, J. Geophys. Res. Atmos., 122, 8739–8760, https://doi.org/10.1002/2017JD026844, 2017.

https://doi.org/10.5194/egusphere-2026-2877
Preprint. Discussion started: 20 July 2026

Grabowski, S. J.: Hydrogen bonding strength - Measures based on geometric and topological parameters, J. Phys. Org. Chem., 17, 18–31, https://doi.org/10.1002/poc.685, 2004.

Harold, S. E., Bready, C. J., Juechter, L. A., Kurfman, L. A., Vanovac, S., Fowler, V. R., Mazaleski, G. E., Odbadrakh, T. T., and Shields, G. C.: Hydrogen-Bond Topology Is More Important Than Acid/Base Strength in Atmospheric Prenucleation Clusters, J. Phys. Chem. A, 126, 1718–1728, https://doi.org/10.1021/acs.jpca.1c10754, 2022.

Herb, J., Nadykto, A. B., and Yu, F.: Large ternary hydrogen-bonded pre-nucleation clusters in the Earth's atmosphere, Chem. Phys. Lett., 518, 7–14, https://doi.org/10.1016/j.cplett.2011.10.035, 2011.

Herb, J., Xu, Y., Yu, F., and Nadykto, A. B.: Large hydrogen-bonded pre-nucleation (HSO4-)(H 2SO4)m(H2O)kand (HSO 4-)(NH3)(H2SO4) m(H2O)k clusters in the Earth's atmosphere, J. Phys. Chem. A, 117, 133–152, https://doi.org/10.1021/jp3088435, 2013.

Höpfner, M., Ungermann, J., Borrmann, S., Wagner, R., Spang, R., Riese, M., Stiller, G., Appel, O., Batenburg, A. M., Bucci, S., Cairo, F., Dragoneas, A., Friedl-Vallon, F., Hünig, A., Johansson, S., Krasauskas, L., Legras, B., Leisner, T., Mahnke, C., Möhler, O., Molleker, S., Müller, R., Neubert, T., Orphal, J., Preusse, P., Rex, M., Saathoff, H., Stroh, F., Weigel, R., and Wohltmann, I.: Ammonium nitrate particles formed in upper troposphere from ground ammonia sources during Asian monsoons, Nat. Geosci., 12, 608–612, https://doi.org/10.1038/s41561-019-0385-8, 2019.

Hu, X., Wu, J., Zhai, Z. H., Zhang, B. Y., and Zhang, J. B.: Determination of gaseous and particulate trifluoroacetic acid in atmosphere environmental samples by gas chromatography-mass spectrometry, Fenxi Huaxue/ Chinese J. Anal. Chem., 41, 1140–1145, https://doi.org/10.1016/S1872-2040(13)60676-3, 2013.

Hu, Y., Chen, S., Ye, S., Wei, S., Chu, B., Wang, R., Li, H., and Zhang, T.: The role of trifluoroacetic acid in new particle formation from methanesulfonic acid-methylamine, Atmos. Environ., 311, 120001, https://doi.org/10.1016/j.atmosenv.2023.120001, 2023.

Hunt, S. W., Higgins, K. J., Craddock, M. B., Carolyn S. Brauer, and and Leopold, K. R.: Influence of a Polar Near-Neighbor on Incipient Proton Transfer in a Strongly Hydrogen Bonded Complex, J. Am. Chem. Soc., 125, 13850–13860, https://doi.org/10.1021/ja030435x, 2003.

Kerminen, V.-M., Wexler, A. S., and Potukuchi, S.: Growth of freshly nucleated particles in the troposphere: Roles of NH3, H2SO4, HNO3, and HCl, J. Geophys. Res. Atmos., 102, 3715–3724, https://doi.org/10.1029/96jd02974, 1997.

Kirkby, J., Curtius, J., Almeida, J., Dunne, E., Duplissy, J., Ehrhart, S., Franchin, A., Gagné, S., Ickes, L., Kürten, A., Kupc, A., Metzger, A., Riccobono, F., Rondo, L., Schobesberger, S., Tsagkogeorgas, G., Wimmer, D., Amorim, A., Bianchi, F., Breitenlechner, M., David, A., Dommen, J., Downard, A., Ehn, M., Flagan, R. C., Haider, S., Hansel, A., Hauser, D., Jud, W., Junninen, H., Kreissl, F., Kvashin, A., Laaksonen, A., Lehtipalo, K., Lima, J., Lovejoy, E. R., Makhmutov, V., Mathot, S., Mikkilä, J., Minginette, P., Mogo, S., Nieminen, T., Onnela, A., Pereira, P., Petäjä, T., Schnitzhofer, R., Seinfeld, J. H., Sipilä, M., Stozhkov, Y., Stratmann, F., Tomé, A., Vanhanen, J., Viisanen, Y., Vrtala, A., Wagner, P. E., Walther, H., Weingartner, E., Wex, H., Winkler, P. M., Carslaw, K. S., Worsnop, D. R., Baltensperger, U., and Kulmala, M.: Role of

https://doi.org/10.5194/egusphere-2026-2877
Preprint. Discussion started: 20 July 2026

sulphuric acid, ammonia and galactic cosmic rays in atmospheric aerosol nucleation, Nature, 476, 429–435, https://doi.org/10.1038/nature10343, 2011.

Koch, U. and Popelier, P. L. A.: Characterization of C-H-O hydrogen bonds on the basis of the charge density, J. Phys. Chem., 99, 9747–9754, https://doi.org/10.1021/j100024a016, 1995.

Kurnig, I. J. and Scheiner, S.: Ab Initio investigation of the structure of hydrogen halide - amine complexes in the gas phase and in a polarizable medium, Int. J. Quantum Chem., 14, 47–56, https://doi.org/10.1002/qua.560320809, 1987.

Kürten, A., Rondo, L., Ehrhart, S., and Curtius, J.: Calibration of a chemical ionization mass spectrometer for the measurement of gaseous sulfuric acid, J. Phys. Chem. A, 116, 6375–6386, https://doi.org/10.1021/jp212123n, 2012.

Kürten, A., Li, C., Bianchi, F., Curtius, J., Dias, A., Donahue, N. M., Duplissy, J., Flagan, R. C., Hakala, J., Jokinen, T., Kirkby, J., Kulmala, M., Laaksonen, A., Lehtipalo, K., Makhmutov, V., Onnela, A., Rissanen, M. P., Simon, M., Sipilä, M., Stozhkov, Y., Tröstl, J., Ye, P., and McMurry, P. H.: New particle formation in the sulfuric acid-dimethylamine-water system: Reevaluation of CLOUD chamber measurements and comparison to an aerosol nucleation and growth model, Atmos. Chem. Phys., 18, 845–863, https://doi.org/10.5194/acp-18-845-2018, 2018.

Lee, S. H., Gordon, H., Yu, H., Lehtipalo, K., Haley, R., Li, Y., and Zhang, R.: New Particle Formation in the Atmosphere: From Molecular Clusters to Global Climate, J. Geophys. Res. Atmos., 124, 7098–7146, https://doi.org/10.1029/2018JD029356, 2019.

Li, Y., Zhang, H., Zhang, Q., Xu, Y., and Nadykto, A. B.: Interactions of sulfuric acid with common atmospheric bases and organic acids: Thermodynamics and implications to new particle formation, J. Environ. Sci. (China), 95, 130–140, https://doi.org/10.1016/j.jes.2020.03.033, 2020.

Lim, X. Z.: There's a new acid in our rain - should we be worried?, Nature, 643, 894–897, 2025.

Lin, Y., Ji, Y., Li, Y., Secrest, J., Xu, W., Xu, F., Wang, Y., An, T., and Zhang, R.: Interaction between succinic acid and sulfuric acid–base clusters, Atmos. Chem. Phys., 19, 8003–8019, https://doi.org/10.5194/acp-19-8003-2019, 2019.

Liu, J., Liu, L., Rong, H., and Zhang, X.: The potential mechanism of atmospheric new particle formation involving amino acids with multiple functional groups, Phys. Chem. Chem. Phys., 23, 10184–10195, https://doi.org/10.1039/d0cp06472f, 2021a.

Liu, L., Kupiainen-Määttä, O., Zhang, H., Li, H., Zhong, J., Kurtén, T., Vehkamäki, H., Zhang, S., Zhang, Y., Ge, M., Zhang, X., and Li, Z.: Clustering mechanism of oxocarboxylic acids involving hydration reaction: Implications for the atmospheric models, J. Chem. Phys., 148, 214303, https://doi.org/10.1063/1.5030665, 2018a.

Liu, L., Li, H., Zhang, H., Zhong, J., Bai, Y., Ge, M., Li, Z., Chen, Y., and Zhang, X.: The role of nitric acid in atmospheric new particle formation, Phys. Chem. Chem. Phys., 20, 17406–17414, https://doi.org/10.1039/c8cp02719f, 2018b.

Liu, L., Yu, F., Tu, K., Yang, Z., and Zhang, X.: Influence of atmospheric conditions on the role of trifluoroacetic acid in atmospheric sulfuric acid–dimethylamine nucleation, Atmos. Chem. Phys., 21, 6221–6230, https://doi.org/10.5194/acp-21-6221-2021, 2021b.

https://doi.org/10.5194/egusphere-2026-2877
Preprint. Discussion started: 20 July 2026

Liu, L., Yu, F., Du, L., Yang, Z., Francisco, J. S., and Zhang, X.: Rapid sulfuric acid-dimethylamine nucleation enhanced by nitric acid in polluted regions, Proc. Natl. Acad. Sci. U. S. A., 118, e2108384118, https://doi.org/10.1073/pnas.2108384118, 2021c.

Liu, Y., Xie, H., Ma, F., Chen, J., and Elm, J.: Amine-enhanced methanesulfonic acid-driven nucleation: predictive model and cluster formation mechanism, Environ. Sci. Technol., 56, 7751–7760, https://doi.org/10.1021/acs.est.2c01639, 2022.

López, S. E. and Salazar, J.: Trifluoroacetic acid: Uses and recent applications in organic synthesis, J. Fluor. Chem., 156, 73–100, https://doi.org/10.1016/j.jfluchem.2013.09.004, 2013.

Lu, T. and Chen, F.: Multiwfn: A multifunctional wavefunction analyzer, J. Comput. Chem., 33, 580–592, https://doi.org/10.1002/jcc.22885, 2012.

Lu, Y., Liu, L., Ning, A., Yang, G., Liu, Y., Kurtén, T., Vehkamäki, H., Zhang, X., and Wang, L.: Atmospheric sulfuric acid-dimethylamine nucleation enhanced by trifluoroacetic acid, Geophys. Res. Lett., 47, e2019GL085627, https://doi.org/10.1029/2019gl085627, 2020.

McGrath, M. J., Olenius, T., Ortega, I. K., Loukonen, V., Paasonen, P., Kurtén, T., Kulmala, M., and Vehkamäki, H.: Atmospheric Cluster Dynamics Code: A flexible method for solution of the birth-death equations, Atmos. Chem. Phys., 12, 2345–2355, https://doi.org/10.5194/acp-12-2345-2012, 2012.

Myllys, N., Olenius, T., Kurtén, T., Vehkamäki, H., Riipinen, I., and Elm, J.: Effect of Bisulfate, Ammonia, and Ammonium on the Clustering of Organic Acids and Sulfuric Acid, J. Phys. Chem. A, 121, 4812–4824, https://doi.org/10.1021/acs.jpca.7b03981, 2017.

Myllys, N., Kubečka, J., Besel, V., Alfaouri, D., Olenius, T., Smith, J. N., and Passananti, M.: Role of Base Strength, Cluster Structure and Charge in Sulfuric Acid-Driven Particle Formation, Atmos. Chem. Phys., 19, 9753–9768, https://doi.org/10.5194/acp-2019-305, 2019.

Nadykto, A., Yu, F., Jakovleva, M., Herb, J., and Xu, Y.: Amines in the Earth's atmosphere: A density functional theory study of the thermochemistry of pre-nucleation clusters, Entropy, 13, 554–569, https://doi.org/10.3390/e13020554, 2011.

Nadykto, A. B. and Yu, F.: Strong hydrogen bonding between atmospheric nucleation precursors and common organics, Chem. Phys. Lett., 435, 14–18, https://doi.org/10.1016/j.cplett.2006.12.050, 2007.

Nadykto, A. B., Yu, F., and Herb, J.: Ammonia in positively charged pre-nucleation clusters: a quantum-chemical study and atmospheric implications, Atmos. Chem. Phys., 9, 4231–4249, https://doi.org/10.5194/acpd-9-4231-2009, 2009.

Narukawa, M., Kawamura, K., Okada, K., Zaizen, Y., and Makino, Y.: Aircraft measurement of dicarboxylic acids in the free tropospheric aerosols over the western to central North Pacific, Tellus B Chem. Phys. Meteorol., 55, 777, https://doi.org/10.3402/tellusb.v55i3.16365, 2003.

Olenius, T., Kupiainen-Määttä, O., Ortega, I. K., Kurtén, T., and Vehkamäki, H.: Free energy barrier in the growth of sulfuric acid-ammonia and sulfuric acid-dimethylamine clusters, J. Chem. Phys., 139, 084312, https://doi.org/10.1063/1.4819024, 2013.

https://doi.org/10.5194/egusphere-2026-2877
Preprint. Discussion started: 20 July 2026

Prevedouros, K., Cousins, I. T., Buck, R. C., and Korzeniowski, S. H.: Sources, fate and transport of perfluorocarboxylates, Environ. Sci. Technol., 40, 32–44, https://doi.org/10.1021/es0512475, 2006.

Stewart, J. J. P.: Optimization of parameters for semiempirical methods V: Modification of NDDO approximations and application to 70 elements, J. Mol. Model., 13, 1173–1213, https://doi.org/10.1007/s00894-007-0233-4, 2007.

Stewart, J. J. P.: MOPAC2016, Stewart Computational Chemistry: Colorado Springs, n.d.

Tian, Y., Yao, Y., Chang, S., Zhao, Z., Zhao, Y., Yuan, X., Wu, F., and Sun, H.: Occurrence and phase distribution of neutral and ionizable per- and polyfluoroalkyl substances (PFASs) in the atmosphere and plant leaves around landfills: A case study in Tianjin, China, Environ. Sci. Technol., 52, 1301–1310, https://doi.org/10.1021/acs.est.7b05385, 2018.

Wang, C., Zhao, J., Chen, X., Zhang, R., and Jiang, S.: Enhancing acid-base-water ternary aerosol nucleation with organic acid: A case of tartaric acid, Phys. Chem. Chem. Phys., 25, 19147–19157, https://doi.org/10.1039/d3cp00809f, 2023.

Wang, M., Kong, W., Marten, R., He, X. C., Chen, D., Pfeifer, J., Heitto, A., Kontkanen, J., Dada, L., Kürten, A., Yli-Juuti, T., Manninen, H. E., Amanatidis, S., Amorim, A., Baalbaki, R., Baccarini, A., Bell, D. M., Bertozzi, B., Bräkling, S., Brilke, S., Murillo, L. C., Chiu, R., Chu, B., De Menezes, L. P., Duplissy, J., Finkenzeller, H., Carracedo, L. G., Granzin, M., Guida, R., Hansel, A., Hofbauer, V., Krechmer, J., Lehtipalo, K., Lamkaddam, H., Lampimäki, M., Lee, C. P., Makhmutov, V., Marie, G., Mathot, S., Mauldin, R. L., Mentler, B., Müller, T., Onnela, A., Partoll, E., Petäjä, T., Philippov, M., Pospisilova, V., Ranjithkumar, A., Rissanen, M., Rörup, B., Scholz, W., Shen, J., Simon, M., Sipilä, M., Steiner, G., Stolzenburg, D., Tham, Y. J., Tomé, A., Wagner, A. C., Wang, D. S., Wang, Y., Weber, S. K., Winkler, P. M., Wlasits, P. J., Wu, Y., Xiao, M., Ye, Q., Zauner-Wieczorek, M., Zhou, X., Volkamer, R., Riipinen, I., Dommen, J., Curtius, J., Baltensperger, U., Kulmala, M., Worsnop, D. R., Kirkby, J., Seinfeld, J. H., El-Haddad, I., Flagan, R. C., and Donahue, N. M.: Rapid growth of new atmospheric particles by nitric acid and ammonia condensation, Nature, 581, 184–189, https://doi.org/10.1038/s41586-020-2270-4, 2020.

Wang, M., Xiao, M., Bertozzi, B., Marie, G., Rörup, B., Schulze, B., and Bardakov, R.: Synergistic HNO3-H2SO4-NH3 upper tropospheric particle formation, Nature, 605, 483–489, https://doi.org/10.1101/pdb.caut449, 2022.

Williamson, C. J., Kupc, A., Axisa, D., Bilsback, K. R., Bui, T. P., Campuzano-Jost, P., Dollner, M., Froyd, K. D., Hodshire, A. L., Jimenez, J. L., Kodros, J. K., Luo, G., Murphy, D. M., Nault, B. A., Ray, E. A., Weinzierl, B., Wilson, J. C., Yu, F., Yu, P., Pierce, J. R., and Brock, C. A.: A large source of cloud condensation nuclei from new particle formation in the tropics, Nature, 574, 399–403, https://doi.org/10.1038/s41586-019-1638-9, 2019.

Wu, J., Martin, J. W., Zhai, Z., Lu, K., Li, L., Fang, X., Jin, H., Hu, J., and Zhang, J.: Airborne trifluoroacetic acid and its fraction from the degradation of HFC-134a in Beijing, China, Environ. Sci. Technol., 48, 3675–3681, https://doi.org/10.1021/es4050264, 2014.

Wu, J., Wang, T., An, M., Ding, S., Yao, B., Western, L. M., Purohit, P., Liu, Z., Zhang, Z., and Peng, L.: Development and validation of a gridded emissions inventory for HFC-134a in China, Environ. Int., 200, 109535, https://doi.org/10.1016/j.envint.2025.109535, 2025.

https://doi.org/10.5194/egusphere-2026-2877
Preprint. Discussion started: 20 July 2026

Xie, G., Cui, J., Zhai, Z., and Zhang, J.: Distribution characteristics of trifluoroacetic acid in the environments surrounding fluorochemical production plants in Jinan, China, Environ. Sci. Pollut. Res., 27, 983–991, https://doi.org/10.1007/s11356-019-06689-4, 2020.

Yao, L., Garmash, O., Bianchi, F., Zheng, J., Yan, C., Kontkanen, J., Junninen, H., Mazon, S. B., Ehn, M., Paasonen, P., Sipilä, M., Wang, M., Wang, X., Xiao, S., Chen, H., Lu, Y., Zhang, B., Wang, D., Fu, Q., Geng, F., Li, L., Wang, H., Qiao, L., Yang, X., Chen, J., Kerminen, V. M., Petäjä, T., Worsnop, D. R., Kulmala, M., and Wang, L.: Atmospheric new particle formation from sulfuric acid and amines in a Chinese megacity, Science, 361, 278–281, https://doi.org/10.1126/science.aao4839, 2018.

You, Y., Kanawade, V. P., De Gouw, J. A., Guenther, A. B., Madronich, S., Sierra-Hernández, M. R., Lawler, M., Smith, J. N., Takahama, S., Ruggeri, G., Koss, A., Olson, K., Baumann, K., Weber, R. J., Nenes, A., Guo, H., Edgerton, E. S., Porcelli, L., Brune, W. H., Goldstein, A. H., and Lee, S. H.: Atmospheric amines and ammonia measured with a chemical ionization mass spectrometer (CIMS), Atmos. Chem. Phys., 14, 12181–12194, https://doi.org/10.5194/acp-14-12181-2014, 2014.

Yu, F. and Luo, G.: Simulation of particle size distribution with a global aerosol model: Contribution of nucleation to aerosol and CCN number concentrations, Atmos. Chem. Phys., 9, 7691–7710, https://doi.org/10.5194/acp-9-7691-2009, 2009.

Zaveri, R. A., Wang, J., Fan, J., Zhang, Y., Shilling, J. E., Zelenyuk, A., Mei, F., Newsom, R., Pekour, M., Tomlinson, J., Comstock, J. M., Shrivastava, M., Fortner, E., Machado, L. A. T., Artaxo, P., and Martin, S. T.: Rapid growth of anthropogenic organic nanoparticles greatly alters cloud life cycle in the Amazon rainforest, Sci. Adv., 8, 1–16, https://doi.org/10.1126/sciadv.abj0329, 2022.

Zhang, B., Zhai, Z., and Zhang, J.: Distribution of trifluoroacetic acid in gas and particulate phases in Beijing from 2013 to 2016, Sci. Total Environ., 634, 471–477, https://doi.org/10.1016/j.scitotenv.2018.03.384, 2018a.

Zhang, H., Li, H., Liu, L., Zhang, Y., Zhang, X., and Li, Z.: The potential role of malonic acid in the atmospheric sulfuric acid - ammonia clusters formation, Chemosphere, 203, 26–33, https://doi.org/10.1016/j.chemosphere.2018.03.154, 2018b.

Zhang, J. and Dolg, M.: ABCluster: The artificial bee colony algorithm for cluster global optimization, Phys. Chem. Chem. Phys., 17, 24173–24181, https://doi.org/10.1039/c5cp04060d, 2015.

Zhang, R., Liu, Y., Yin, R., Ma, F., Xia, D., Chen, J., Xie, H. Bin, and Francisco, J. S.: Significance of halogen bonding in the synergistic nucleation of iodine oxoacids and iodine oxides, Chem. Sci., 16, 15935–15946, https://doi.org/10.1039/d5sc02517f, 2025.

Zhao, Y. and Truhlar, D. G.: The M06 suite of density functionals for main group thermochemistry, thermochemical kinetics, noncovalent interactions, excited states, and transition elements: Two new functionals and systematic testing of four M06-class functionals and 12 other function, Theor. Chem. Acc., 120, 215–241, https://doi.org/10.1007/s00214-007-0310-x, 2008.

Zhao, Y. and Truhlar, D. G.: Applications and Validations of the Minnenesota Density Functionals, Chem. Phys. Lett., 502, 1–13, https://doi.org/10.1016/j.cplett.2010.11.060, 2011.

https://doi.org/10.5194/egusphere-2026-2877
Preprint. Discussion started: 20 July 2026

Zheng, J., Yang, D., Ma, Y., Chen, M., Cheng, J., Li, S., and Wang, M.: Development of a new corona discharge based ion source for high resolution time-of-flight chemical ionization mass spectrometer to measure gaseous H2SO4 and aerosol sulfate, Atmos. Environ., 119, 167–173, https://doi.org/10.1016/j.atmosenv.2015.08.028, 2015.

590